PAPER

Check for updates

Polymer-loaded hydrogels serve as depots for lactate and mimic "cold" tumor microenvironments†

Riley Allen, Emilie Ivtchenko, Bhasirie Thuamsang, Rapeepat Sangsuwan and Jamal S. Lewis [ID] *

The burgeoning field of biomaterials for immunotherapy has aided in the understanding of foundational mechanisms of cancer immunology. In particular, implantable biomaterials can be engineered to investigate specific aspects of the tumor microenvironment either singularly or in combination. Of note, the metabolite – lactate, a byproduct of anaerobic glycolysis, is known to reprogram immune cells, resulting in increased tumor survival. An adequate model that can recapitulate intratumoral lactate concentrations does not exist. In this study, we demonstrate that a simple biomaterial platform could be developed as an instructive tool to decipher the effects of lactate *in vivo*. Briefly, we demonstrate that a peptide hydrogel loaded with granulocyte-macrophage colony stimulating factor and poly-(lactic-*co*-glycolic acid)/(lactic acid) microparticles can generate the localized lactate concentrations (∼2–22 mM) and cellular makeup of the tumor microenvironment, following subcutaneous implantation in mice. Furthermore, infiltrating immune cells adopt phenotypes similar to those seen in other *in vitro* and *in vivo* cancer models, including immunosupressive dendritic cells. This hydrogel system is a framework to interrogate immune cell modulation in cancer-like environments using safe and degradable biomaterials. Moreover, this system can be multifaceted, as incorporation of other cancer tumor environmental factors or chemotherapeutic drugs is facile and could be insightful in developing or improving immunotherapies.

Introduction

Recent advances in the field of cancer immunology have spurred a tidal wave of immunotherapeutics which are now available to clinicians for fighting previously untreatable cancers. Unlike traditional chemotherapies, immunotherapy engages the body's natural immune response to defeat a malignant mass.[1] Immunotherapeutic approaches are effective by either harnessing the ability of the host immune system to recognize and eliminate cells that display tumor antigens, providing external inflammatory stimuli to induce the destruction of tumor cells in an antigen-specific manner, or by negating the ability of the tumor cells to inhibit host immune cell activation. The latter strategy is particularly attractive as it avoids constitutive activation of immune cells, which can result in collateral damage to healthy tissues.[2] Moreover, this strategy can be accomplished by regulating molecular signals within the tumor microenvironment (TME) to shift tumors from

being "immunologically cold" and immune-evasive, to "immunologically hot" and susceptible to detection and elimination by immune elements.[3] For instance, checkpoint inhibitor therapies, like Keytruda® (anti-PD-1), increase tumor susceptibility to immune attack through monoclonal antibodies that bind and block the actions of inhibitory molecules (PD-1) on invading lymphocytes.[2] Checkpoint inhibitory therapies have been relatively successful – the rate of long term remission for patients on this type of therapy ranges from 25–35% based on the cancer type.[4] Although this is a substantial improvement over more conventional therapies, it still fails to rid the patient of tumor burden in a number of cases. This is thought to be due to the fact that the patient's tumor remains "cold" and non-immunogenic. Additionally, these therapeutics remain wildly expensive to manufacture and administer. As such, active research is now underway to uncover other molecules that may play a critical role in maintaining the 'cold' climate of the TME. One molecule that is ubiquitous in the TME and now emerging as source of immune suppression is lactate.

Lactic acid is an intermediate in glucose metabolism and at physiological pH is found as the conjugate base, lactate. Lactate is surprisingly both a byproduct and energy source for cancer cells, depending on the availability of oxygen.[5]

Department of Biomedical Engineering, University of California (Davis), Davis, CA 95616, USA. E-mail: jamlewis@ucdavis.edu
†Electronic supplementary information (ESI) available. See DOI: 10.1039/d0bm01196g

Traditionally, tumors were described as glucose avid tissues that produce lactate despite adequate oxygen tension, colloquially known as the "Warburg effect".[6] However, recent research aided by next generation sequencing has revealed that this is not the complete metabolic picture, and in fact, there is evidence of a "Reverse Warburg effect", whereby stromal cells produce lactate that tumor cells take up and oxidize.[6]

Regardless of its role in metabolism, lactate serves as a potent immune signaling molecule. Within the TME, lactate drives the differentiation of immunosuppressive cell subsets, such as pro-tumorogenic dendritic cells (DCs), which characteristically decrease their costimulatory potential and have the ability to expand regulatory networks (e.g. regulatory T cells), thereby halting subsequent anti-tumor adaptive immune responses.[7,8] Lactate also impairs the differentiation of monocytes into macrophages (MΦ) and DCs and the lipopolysaccharide (LPS)-induced maturation of MΦs and DCs in the TME.[9,10] Furthermore, lactate inhibits lymphoid cells, mainly NK and T cells, the primary cytotoxic responders to cancer. Though not universal for every tumor, the accumulation of lactate in the TME causes a reduction in intracellular pH leading to mitochondrial dysfunction and apoptosis of invading T and NK immune cells.[11–13]

These groundbreaking studies have highlighted the importance of immunometabolism and, specifically lactate on the host's immune response to cancer. Despite the importance of this molecule to cancer biology, we lack a defined model that replicates lactate conditions seen in the TME. In vitro models of solid tumors range from tumor-derived cell lines to 3D models of the TME, but vary in complexity and consistency.[14] Further, these models often fail to recapitulate the complex milieu of immune factors and immune cells that are present in the in vivo setting and crucial for mechanistic discovery and evaluation of immunotherapies. Although in vivo models, such as patient-derived xenografts, have been shown comparable concentrations of lactate as seen in human tumors, the phenotypes of immune cells in in vivo models are prejudiced by a multitude of factors.[15] Succinctly, current cancer models fail to isolate the effects of lactate, as well as other molecules that may be of interest to cancer immunologists, including immuno modulatory drugs. Moreover, a combinatorial model, where lactate can be incorporated in combination with other molecules/conditions of interest (e.g. hypoxia) is highly desired.

Engineered biomaterial constructs may offer a clever solution for this need. Biomaterials have been exploited to identify and recreate specific aspects of the tumor stroma, for example – stiffness, topography and nutrient exchange.[16] Using biomaterials allows for the fabrication of reductionist systems to study basic mechanisms that regulate cancer cell plasticity, dissemination and repopulation of the niche. Collagen gels were first used as 3D scaffolds to demonstrate how normal murine mammary epithelial cells form lumens in 3D as opposed to monolayers on 2D substrates, emphasizing the importance of 3D materials to recreate in vivo cell morphologies in vitro.[17] Building on this notion, and as evidence of the power of biomaterials to isolate single components in

the TME, Bersani et al. showed that bioengineered polyacrylamide scaffolds could be used to dissect the cellular components that contribute to metastasis.[18] Of note, this work showed that the cytokine, IL-1β, was a key factor in promoting tumor cell engraftment during metastasis.

Herein, we engineered a TME-mimicking system that is able to replicate a critical component of the TME, endogenous lactate levels, to understand the direct effect of localized lactate concentrations on immune cells. This system utilizes peptide hydrogels loaded with granulocyte macrophage-colony stimulating factor (GM-CSF) and degradable lactate-based polymers. The hydrogel environment encapsulates the polymer in a hydrated peptide mesh which allows for its hydrolysis into monomeric lactate and the subsequent accumulation of lactate in the hydrogel. Additionally, GM-CSF, a suppressive secretory chemokine produced by many tumors, serves to recruit innate immune cells, primarily, DCs and MΦs, to the hydrogel and blocks antigen-specific immunity towards the tumor.[19] Tunable parameters, including the lactate concentration in the hydrogel, were investigated for their immunomodulatory effects. Directly uncovering the isolated effects of lactate on immune cells in vivo may provide evidence for targeting this molecule as an immunotherapeutic strategy. Additionally, this platform is expandable to potentially include other tumor-resident immunomodulatory agents for combinatorial investigation.

Materials methods

Experimental animals

Both male and female C57BL/6J and BALB/cByJ mice were purchased from Jackson Laboratories. All animals were housed in specific pathogen-free environment conditions at the University of California, Davis TRACS facility. All animal procedures were performed in accordance with the Guidelines for Care and Use of Laboratory Animals of the University of California, Davis, and approved by the UC Davis Institutional Animal Care and Use Committee.

Fabrication of lactate-releasing microparticles

Several different poly-(lactic-co-glycolic acid) (PLGA) compositions with differing molecular weights were purchased from commercial sources to serve as depots of lactate with differing hydrolysis rates. Two PLGA polymers with a 50 : 50 ratio of individual monomers (Corbion, Netherlands) and differing molecular weights 5002 (PURASORB PDLG 5002A, ~10 kDa, acid terminated), and 5010 (PURASORB PDLG 5010, ~90 kDA, ester terminated), and an acid-terminated poly(D,L-lactic acid) (PLA; M_w ~10 kDa) (PURASORB PDL 02A) were used. Henceforth, these formulations are referred to as 5002, 5010, and PLA, respectively. To make phagocytostable microparticles (MPs), the PLGA and PLA polymers were dissolved in dichloromethane (DCM) (Fisher Scientific, New Jersey, United States) at 5% w/v ratio. For fluorescently-labeled MPs, 50 μL of a 5 mM 1,1-dioctadecyl-3,3,3,3-tetramethylindodicarbocyanine

(DiD) solution (AAT Bioquest, Sunnyvale, CA) was co-dissolved with 5002, 5010, or PLA in DCM. This solution was added to 2 mL of 5% poly(vinyl alcohol) (PVA; Fisher Scientific; 87% hydrolyzed, M_w ~100 000 g mol^{-1}) solution in diH$_2$O and homogenized at 35 000 rpm for 180 s using a Tissuemiser homogenizer (OMNI, Kennesaw, GA) to form a primary emulsion. This solution was added to 30 mL of 1% PVA solution. The MPs thus formed were agitated using a magnetic stirrer (Fisher Scientific) for 24 h to evaporate residual DCM. The remaining solution was centrifuged at 10 000g for 15 min to collect MPs. The pelleted MPs were subsequently washed three times with diH$_2$O. The water was aspirated from the centrifuged MPs on the final wash, and the remaining pellet was lyophilized overnight. The MPs were stored at −20 °C until use. Green fluorescent polystyrene (PS) particles (1.0 μm) were purchased from Thermo Fisher. The microparticle hydrodynamic diameter was determined using Malvern ZetaSizer Nano ZS (Malvern Instruments, UK).

Preparation of MP-loaded or unloaded peptide hydrogels

The PuraMatrix™ peptide was sourced from the manufacturer (BD Biosciences) as a 1.0% (w/v) solution at pH 2.0–2.5. In order to help stabilize the hydrogel-incorporated components in acidic pH, the peptide solution was mixed with 10% sterile sucrose (Fisher Scientific). For experimental groups which included MPs, a desired mass of the lyophilized MPs was then mixed with the peptide/hydrogel solution. Stock solutions of recombinant mouse GM-CSF (R&D systems, Minneapolis, MN, USA) in sterile PBS (1 mg mL^{-1}) were prepared. To form the injectable GM-CSF/MP-loaded hydrogel, 5 mg of either 5002, 5010, PLA, or PS MPs were sonicated in 100 μl of PBS. In a separate container 1 μL of 1 mg mL^{-1} of GM-CSF (R&D systems) in PBS was added to 9 μL of 10% sterile sucrose. The buffered GM-CSF solution was then mixed with 90 μL of the stock PuraMatrix™ solution and quickly drawn into a 1 mL syringe through a 20 gauge needle. The MP solution was drawn into the syringe thereafter and mixed with the peptide solution by dispensing and redrawing the solution into the syringe. The GM-CSF laden hydrogel loaded with either 5002, 5010, PLA, or PS MPs will be referred to as hyd-5002, hyd-5010, hyd-PLA, or hyd-PS respectively.

GM-CSF release from the hydrogel

To quantify the concentration of GM-CSF released in the hydrogel environments, 10 μg of GM-CSF, 5 mg of 5002, 5010, or PLA polymeric MPs were loaded into 100 μl of hydrogel at the base of a 12 well plate. Following addition of PBS with calcium and magnesium, the plates were left untouched for 10 minutes for the hydrogel to polymerize. After polymerization, 5×10^6 splenocytes from BALB/cByJ mice in 2 ml of RPMI medium with L-glutamine and 25 mM HEPES (Mediatech, Manassas, VA) containing 10% fetal bovine serum (FBS) (Mediatech) and 1% penicillin/streptomycin were added and incubated at 37 °C in 5% CO$_2$.[20] At 1, 4, 7, and 14 days the supernatants were tested for GM-CSF concentrations via a mouse GM-CSF ELISA (R&D systems).

Lactate quantification and cell viability

To quantify the concentration of lactic acid in the hydrogel environments, 1, 5, or 10 mg of 5002, 5010, or PLA polymeric MPs were loaded into 100 μl of hydrogel at the base of a 12 well plate. Following addition of PBS with calcium and magnesium, the plates were left untouched for 10 minutes for the hydrogel to polymerize. After polymerization, 5×10^6 splenocytes from BALB/cByJ mice in 2 mLs of RPMI medium with L-glutamine and 25 mM HEPES (Mediatech, Manassas, VA) containing 10% FBS (Mediatech) and 1% penicillin/streptomycin were added and incubated at 37 °C for the designated time points.[20] Cell viability was assessed by lysing the hydrogel in PBS and collecting all the cells from the culture environment. Cells were subsequently stained with DiD and cell death was quantified using Zombie UV fixable viability kit (Biolegend) according to the manufacturer's instructions. Lactate was quantified using the Megazyme D,L-lactic acid assay kit according to manufacturer's instructions. Samples were deproteinised before the assay by adding an equal volume of ice-cold 1 M perchloric acid. Following, samples were centrifuged at 1500g for 10 min and the supernatant was neutralized with 1 M KOH.

Dendritic cell enrichment in injected hydrogels

To investigate DC enrichment in the hydrogel injection site, 90 μL of PuraMatrix™ peptide hydrogel solution was combined with 10 μL of GM-CSF solution (1 mg mL^{-1} in PBS) or 10 μL of PBS. The subsequent solution was injected subcutaneously into the left side of the upper abdominal region of C57BL/6J mice. After 1, 4, 7, and 14 days mice were euthanized, and the injected hydrogel was excised and homogenized over a 70 μm cell strainer. The subsequent single cell suspension was then washed with 1% FBS in PBS and incubated in a 1 μM DiD solution in PBS. The DiD-stained cells were washed twice with PBS and incubated with antibodies against CD16/CD32 (Fcγ III/II receptor) (clone 2.4G2, IgG2b, k); (BD Pharmingen, CA, United States) in 1% FBS for 15 min at 4 °C to block Fcγ receptors. Cells were washed and then stained with antibodies against CD11c (clone HL3, IgG1, l2) for 30 min at 4 °C. Data acquisition was performed using (Attune NxT, Life Tech) flow cytometry. Percentages of DCs in the hydrogels was determined by the percentage of CD11c+DiD+ events.

Immune cell type and phenotype

To ascertain the immune cell (DCs, MΦs, B cells, and T cells) composition of the hydrogel (with respect to time), as well as their immune phenotype, MP-loaded hydrogels were injected into the left flank of C57BL/6J mice. After either 1, 4, 7, or 14 days, the inguinal lymph node (iLN), popliteal lymph node (pLN), brachial lymph node (bLN), spleen, and remaining hydrogel at the injection site were excised and homogenized into separate single cell suspensions. After blocking Fcγ receptors as described previously, cells were stained with antibodies against CD11c (clone HL3, IgG1, l2), I-A/I-E (clone M5/114.15.2, IgG2b, κ), CD86 (clone GL1, IgG2a, κ), F4/80 (clone

T45-2342, IgG2a, κ), CD3 (clone 17A2, IgG2b, κ), CD28 (clone 37.5, IgG), CD40L (clone MR1, IgG$_3$, κ), CD19 (clone 6D5, IgG2a, κ), CD40 (clone 3/23, IgG2a, κ) and analyzed as previously described.

Statistical analysis

Statistical analyses were performed using a repeated measure two-way ANOVA for all experiments with multiple time points. For experiments performed at only one time point, one-way ANOVAs were used. Statistical significance was determined by *post hoc* pairwise comparisons using Tukey tests. For pairwise comparisons, the means of each treatment group were compared. Differences were considered significant if $p \leq 0.05$ using the Prism software (Version 7, GraphPad, La Jolla, CA).

Results and discussion

Despite many advances in mimicking the TME, few models are able to recapitulate the immunological "coldness" seen at the advanced stage cancer.[21] The gold standard of *in vivo* models, tumor xenografts, are valuable for understanding systemic responses to tumors, but fail in delineating the underpinnings of therapeutic efficacy and the dynamics of specific protumor factors over the course of therapy. Moreover, the contribution of immune cells, which are important constituents of the TME and determinative of tumor destruction or survival, are often neglected in current models.[22,23] Beneath the backdrop of tumor cells exists a vast, complicated, and dynamic system of immune cells, cytokines, growth factors, metabolites and matrix remodeling enzymes that makeup the TME.

One emerging immunomodulatory molecule of interest in the TME is lactic acid, or rather, its anion lactate. There is now growing evidence that lactate, produced in excess by cancer cells, favors tumor growth and metastasis.[24] Lactate exerts this effect, at least in part, by disrupting the normal antitumor function of certain immune cells to create an immunosuppressive TME. Found at concentrations as high as 40 mM, lactate effectively inhibits a majority of T cell anti-tumoral activities, including proliferation and cytokine production by up to 95%, and cytotoxic activity up to 50%.[25] Alone, lactate is a powerful immunomodulator, but the TME is full of other factors, including cytokines and growth factors, which adds complexity to the immunomodulatory properties of the TME.

For instance, GM-CSF is a prominently secreted chemokine in several tumors that promotes tumor growth and metastasis.[26] Perhaps best known for its critical role in immune modulation and hematopoiesis, GM-CSF exerts all of its biological activities by binding and activating its cognate heteromeric receptor (also known as CD116), which is present on multiple cell types, including endothelial cells, granulocytes, lymphocytes, MΦs and monocytes.[26] Evidence suggests that GM-CSF can inhibit anti-tumor activity, either by polarizing T cells towards Th2 phenotypes or by altering the stroma (white adipose tissue) in adipose rich cancers, such as breast cancer, to a tumor-supportive environment.[27,28]

Evidently, these two molecules are critical in instructing the modulation of tumor-resident immune cells. We hypothesized that a biomaterial-based construct could be developed to answer some of the systems biology questions pertaining to lactate (initially) in the context of the tumor. To mimic the immunomodulatory properties of the TME, we encapsulated GM-CSF, along with phagocytosable, lactide, polymeric MPs (PLA or PLGA), into a peptide-based hydrogel. The hydrogel environment allowed for controlled release of both lactate and GM-CSF which led to immune cell recruitment and immunomodulation of key immune cells after subcutaneous implantation into C57BL/6J mice. We propose that the combination of a hydrogel and source of lactate provides a localized chemical milieu to study the effect of lactate on immune cells. We investigated this concept by first characterizing the release of GM-CSF from the hydrogel.

GM-CSF release results in DC migration into the hydrogel

The release of GM-CSF from the PuraMatrix™ hydrogel in culture with splenocytes followed a burst release pattern with the majority of the release occurring in the first 24 h (Fig. 1A). Moreover, by 14 days, 95 ± 7.6% release of the loaded GM-CSF is achieved across all formulations (excluding the hydrogel alone), indicating that most of the payload is released into the *in vitro* environment. Hydrogel-loaded GM-CSF was released in a relatively quick fashion compared to other GM-CSF delivery devices, such as PLGA scaffolds, where slower cummulative release over time was observed.[29] However, the release of GM-CSF in our TME-mimicking system was similar to other protein/peptide delivery using the PuraMatrix™ platform, which report almost 100% release of encapsulated protein after 12 hours in the cellular environment.[30]

We then investigated the capacity of GM-CSF-laden hydrogels to chemotactically recruit DCs to the site of injection and into the hydrogel, we loaded GM-CSF into the peptide hydrogels and injected them subcutaneously into C57BL/6J mice. Granulocyte macrophage-colony stimulating factor was effective at recruiting DCs to the injection site, particularly after 1 week (Fig. 1B). We observed significant increases in the number of CD11c+ stained cells at the injection site of GM-CSF-laden hydrogels compared to the hydrogel only at both 7 and 14 days post injection. At shorter incubation times, there were no significant differences in DC populations, which is incongruous with our *in vitro* release kinetics data. Of course, *in vivo* release, which was not assessed, could be different from that observed in the petri dish. Additionally, the acute inflammatory response at the injection site could play a role in cell infiltration of the biomaterial, possibly masking the effects of additional chemokine(s) at early time points.[31] Nevertheless, our overall results on DC migration due to GM-CSF supplementation are consistent with other studies, including those recounted by Miller *et al.* This group reported that DCs peaked in population in the spleen 7 days after i.v. administration of GM-CSF.[32] Moreover, Sivakumar *et al.* highlighted the increased population of tumor-associated DCs over 7 days in a subcutaneous syngeneic breast cancer cell line.[33]
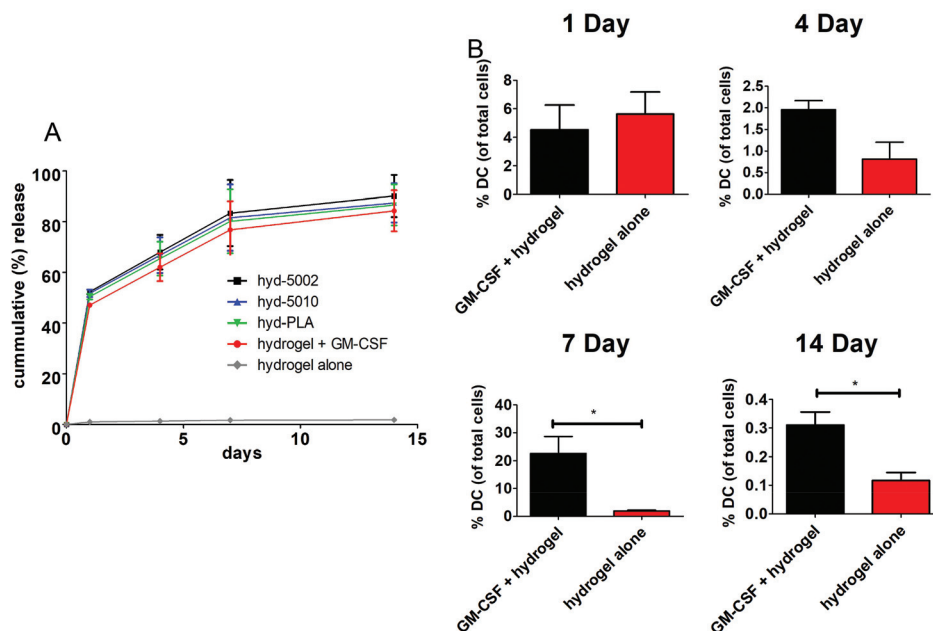
Fig. 1 GM-CSF laden hydrogels release GM-CSF into the environment and increase the percentage of dendritic cells in injection site. (A) Peptide hydrogels were loaded with 10 μg of GM-CSF and cultured with 5×10^6 splenocytes in culture media or injected subcutaneously into C57BL/6J mice. GM-CSF release from the hyd-5002, hyd-5010, and hyd-PLA was quantified in culture after 1, 4, 7, and 14 days incubation. Percent release of total loaded mass of GM-CSF is shown. GM-CSF was quantified via ELISA. (B) Peptide hydrogels were loaded with 10 μg of GM-CSF and injected subcutaneously into C57BL/6J mice. The injection site was then extracted 1, 4, 7, and 14 days post-injection. DC populations, as defined by CD11c expression, in the hydrogel were quantified using flow cytometry. Histograms represent mean and standard error. The * represents a significant difference between cell number $p < 0.05$ ($n = 3$ biological replicates for each time point).

One last noteworthy observation in our results is the flux of DCs in the hydrogels over the 14-day period. This is likely the manifestation of DC invasion and emigration from the hydrogel, regulated by GM-CSF presence.[34] Ostensibly, the GM-CSF-laden hydrogel closely models the increase in DC populations seen in tumors.

The hydrogel environment creates localized TME-mimicking lactate concentrations

We propose that is this hydrogel system can be used as an investigative tool to probe the effects of lactate on invading immune cells in the TME. The Warburg effect is one of the main contributors to the accumulation of lactate in the TME. Importantly, the Warburg phenotype has been associated, not only with an increased energy demand, but also with the activation of numerous transcription factors, such as c-Myc, nuclear factor kappa-light-chain-enhancer of activated B cells (NF-κB), and hypoxia-inducible factor 1-α. These transcription factors can regulate the expression of metabolic enzymes resulting in the deregulated conversion of glucose to lactate, thereby promoting a "tumor lactagenesis" state.[24] Ultimately this leads to high concentrations of lactate compared to normal physiological levels. The concentration of lactate in blood and healthy tissues is about 1.5–3 mM, but in cancer tissues it can be present at concentrations as high as 10–40 mM.[24]

To justify the use of this engineered biomaterial platform for this application, we quantified the concentration of lactate within the hydrogel at 1, 4, 7, and 14 days. Furthermore, to investigate the optimum mass of MPs in hydrogels to achieve concentrations of lactate comparable to known intratumoral concentrations, we varied the mass of MPs loaded and the molecular weight of the polymer, which are relevant to the concentration and release rates of lactate.[37]

In general, lactate concentrations increased over time in the hydrogel environment (Fig. 2). After 24 h, for the hydrogels containing 5 mg of MPs, lactate levels in the hyd-5002 were significantly higher than that of the hydrogel alone and hyd-5010. The pattern of lactate accumulation varied based on the mass of MPs loaded, starting at 4 days. In the hydrogels containing 10 mg of MPs, the hyd-5002 had statistically significantly higher lactate concentrations than all other formulations. In the hydrogels with 5 mg of MPs, all MP-loaded hydrogels had statistically higher levels of lactate compared to the hydrogel without MPs at the 4-day time point. Interestingly, we observed a similar trend at 7 days in the hydrogels with 5 mg of hydrogels loaded with 10 mg at 4 days, where the hyd-5002 had significantly higher lactate concentrations compared to all other formulations. After 7 days of incubation, in the hydrogels with 10 mgs of MP, there were significantly higher concentrations of lactate in the hyd-5002 and hyd-PLA compared to the hydrogel + GM-CSF (with no MPs). Finally, after 14 days of incubation, for hydrogels loaded with
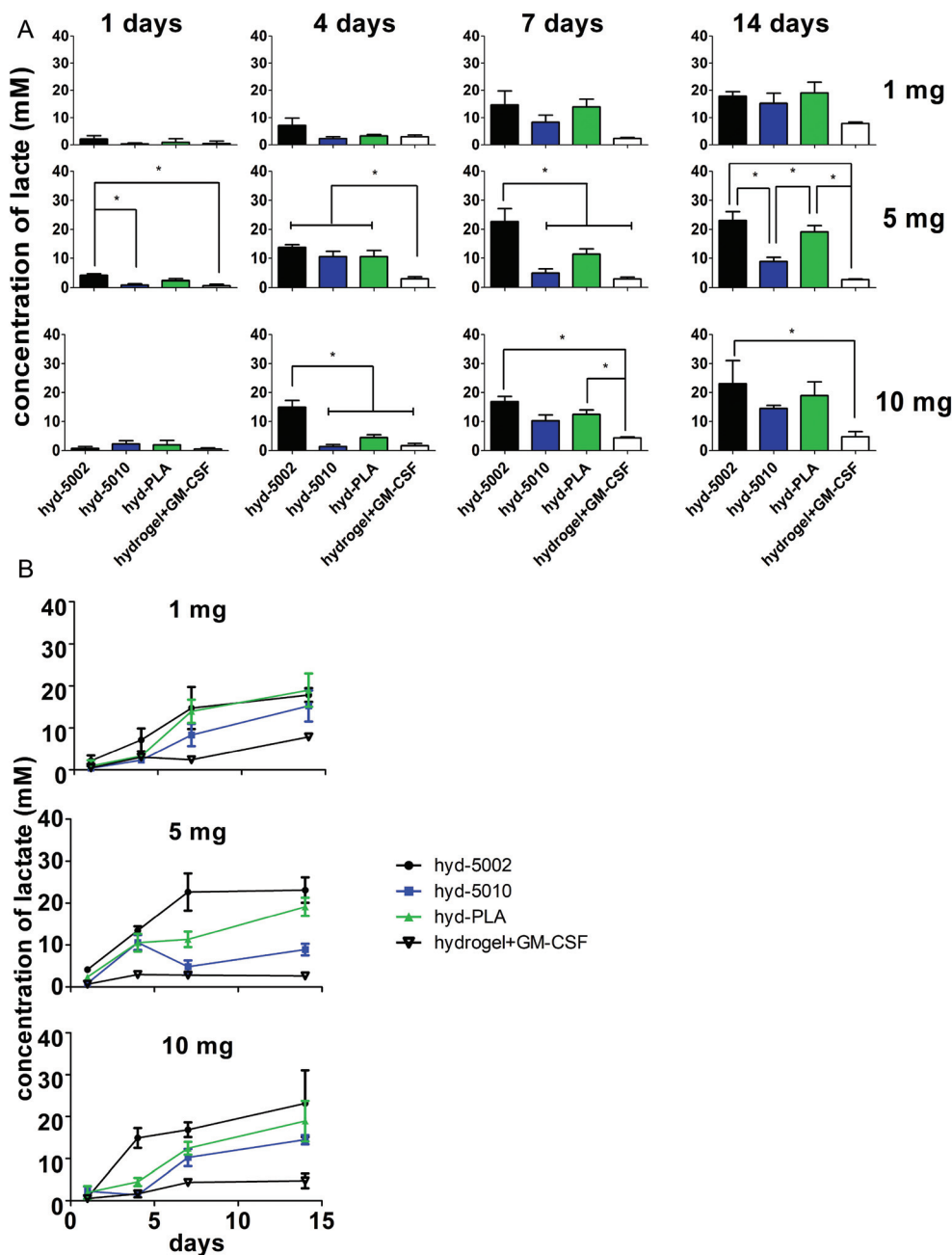
Fig. 2 Lactate in the hydrogel increases in concentration over time with the influx of cells and hydrolysis of PLGA/PLA MPs in the aqueous environment. The extracellular D,L-lactate concentration in the homogenized hyd-5002, hyd-5010, hyd-PLA formulations loaded with either 1, 5 or 10 mg of MPs was measured using an enzyme-based colorimetric assay by collecting the hydrogels from culture at 1, 4, 7 and 14 days with splenocytes, pelleting any free particles by centrifugation at ~10 000g, and assaying for lactate with an enzymatic-based detection kit. (A) Histograms represent mean and standard error. The * symbol represents a pairwise significance difference ($p < 0.05$; $n = 3$ biological replicates per formulation per time point). Significance was determined using two-way ANOVA of the entire data set followed by comparisons of the means of each treatment group at each time point using a *post hoc* Tukey test. (B) The same dataset is displayed in an alternative x,y format to highlight the lactate accumulation over time.

5 mg MPs, both the hyd-5002 and hyd-PLA had significantly higher lactate levels compared to the hyd-5010 and hydrogel + GM-CSF respectively. In the hydrogels loaded with 10 mg only the hyd-5002 had higher concentrations compared to the hydrogel with GM-CSF alone, at the final time point.

Comparing intra-hydrogel lactate concentration across MP mass, we observed significantly higher lactate levels after 4 days in the 5 mg loaded hydrogels compared to the 10 and 1 mg loaded hydrogels in the hyd-5010 (Fig. S2†). Moreover, at 4 days, the total lactate concentrations approached 10 mM,

which is akin to concentrations recorded in head, neck and cervical cancers. Concentrations seen at the later timepoints approached 22 mM, consistent with the high lactate levels seen in mouse xenografts and some human cancers.[24] It should also be noted that the Young's modulus of these peptide hydrogels closely resembles that seen in late stage tumors (13–15 kPa).[35,36] Therefore, we are creating an environment that mimics both the biochemical and biophysical characteristics of the TME.

For further investigation in mice, we selected the 5 mg of MPs quantity for loading into hydrogels, as *in vitro* it showed the greatest variability in lactate production between different polymer types. This could be critical for mimicking the TME of various cancer types. Additionally, 5 mg MPs was previously used in a similar system, albeit for a different immune modulatory application.[20]

Hydrogel innate and adaptive immune cell composition similar to the TME

Immune cell composition in the TME is an important prognostic marker for the efficacy of immunotherapy.[38] As tumors transition from the initiation phase to the malignant phase, key immunophenotypically-distinct immune cells rise in abundance.[39] In general, increased cellular infiltration corresponds with better outcomes for human patients. As such, we profiled the cellular makeup of the hydrogel environment by assaying four general, immune cell types, DCs, MΦs, B cells, and T cells, following hydrogel implantation.

After 1, 4, 7, and 14 days of incubation in C57BL/6J mice with either hyd-5002, hyd-5010, hyd-PLA, or hyd-PS, the injection site was extracted and cells were stained for CD11c, F4/80, CD19, and CD3 to identify DCs, MΦs, B cells and T cells respectively. We used a hydrogel alone (without GM-CSF) as a control in this experiment. Polystyrene MPs were used as a non-degradable and non-lactate-releasing polymer control. Without the addition of GM-CSF and polymer to the hydrogel, we observed low levels of innate immune cells in the injection site. With the addition of GM-CSF and polymeric MPs, the cellular composition in the hydrogel changed dramatically (Fig. 3). Specifically, we observed significantly more DCs at 7 and 14 days in the hyd-5002 and hyd-PLA, compared to the hydrogel alone. Moreover, when comparing the degradable, lactate-releasing hydrogels with the non-degradable, PS-loaded hydrogel, we observed significantly higher DC frequency in the hyd-5002 and hyd-PLA formulations. Interestingly, the number of MΦs were significantly increased in the hyd-PS compared to the hydrogel alone after 7 days of incubation.

The higher percentages of DCs observed in the hyd-5002 and hyd-PLA compared to the hydrogel alone at 7 and 14 days can be attributed to the cummulative release of GM-CSF to the hydrogel microenvironment.[20] The trafficking of B cells and T cells was not altered by the particulate formulation or the addition of GM-CSF. The composition of immune cells in the hydrogels represents the dynamic changes seen in immune surveillance of tumors.[40] Previous reports in this area have demonstrated that there is infiltration of the TME by immune cells in a wave-like pattern. The first wave is composed of T cells, including an abundant population of Th17 cells. This first-line wave is followed by an increased presence of MΦs and DCs.[40] The hydrogel was able to replicate this pattern in the majority of the formulations highlighting the feasibility of this system to mimic important cellular dynamics.

Lactate-releasing, MP-loaded hydrogels modulate innate immune cell maturation status

Central to our hypothesis is the demonstration of immunomodulation by lactate-producing hydrogels. For this purpose, we scrutinized both innate and adaptive immune cells at the implant site and the immediate draining lymph node (inguinal lymph node). We previously demonstrated that PLGA MPs have latent, immunosuppressive effects on DCs.[41] The driving force behind these immunosuppressive effects was the accumulation of lactate, which results in the inhibition of NF-κB activity. Our current findings align with this previous report (and others), which was performed *in vitro*.

Our previous findings focused on the maturation status of DCs exposed to lactate in co-culture with PLGA MPs. In this study, we again looked at the maturation status of innate immune cells exposed to lactate in the context of the TME-mimicking, hydrogel. In these analyses, we phenotyped both the particle-associated and particle-free cells from the injection site. If events were double positive for the cell marker and particle fluorescence (CD11c, F4/80 and DiD or FITC), they were classified as particle-associated. To simplify the analysis and comparison between treatment groups, we employed the '*in vivo* relative index', which describes the number of DCs or MΦs positive for each maturation marker (*e.g.* # CD86+CD11c+) divided by the total number of each cell type (*e.g.* # CD11c+).

Summarily, DC maturation was altered in the PLGA- and PLA-loaded hydrogels when compared to the non-degradable, PS-loaded hydrogels (Fig. 4A). However, there were different patterns of maturation in all DCs at the injection site, as well as particle-associated DCs at the injection site. For total DCs resident at the injection site, we observed differences in CD86 expression at 4, 7, and 14 days of hydrogel incubation. At days 4 and 7, the trends in CD86 expression were similar – the hyd-PLA, hyd-5002, and hyd-5010 hydrogels had decreased CD86 expression compared to the hyd-PS and hydrogel alone controls. Whilst only the hyd-5002 had decreased CD86 expression on DCs after 14 days of incubation, compared to the hyd-PS.

We also investigated the particle-associated DCs, which were identified based on positive fluorescence for both the particles and the CD11c+ marker. This subset of DCs in the injection site showed earlier signs of decreased CD86 expression. For instance, after 24 h, particle-associated DCs from the injection site from hyd-5002 and hyd-PLA showed decreased CD86 expression compared to hyd-PS. At 7 days all degradable MP-loaded hydrogel formulations induced significantly lower CD86 expression compared to hyd-PS. However, after 14 days of incubation, we observed no difference in maturation status of particle-associated DCs between hyd-5002, hyd-5010, hyd-
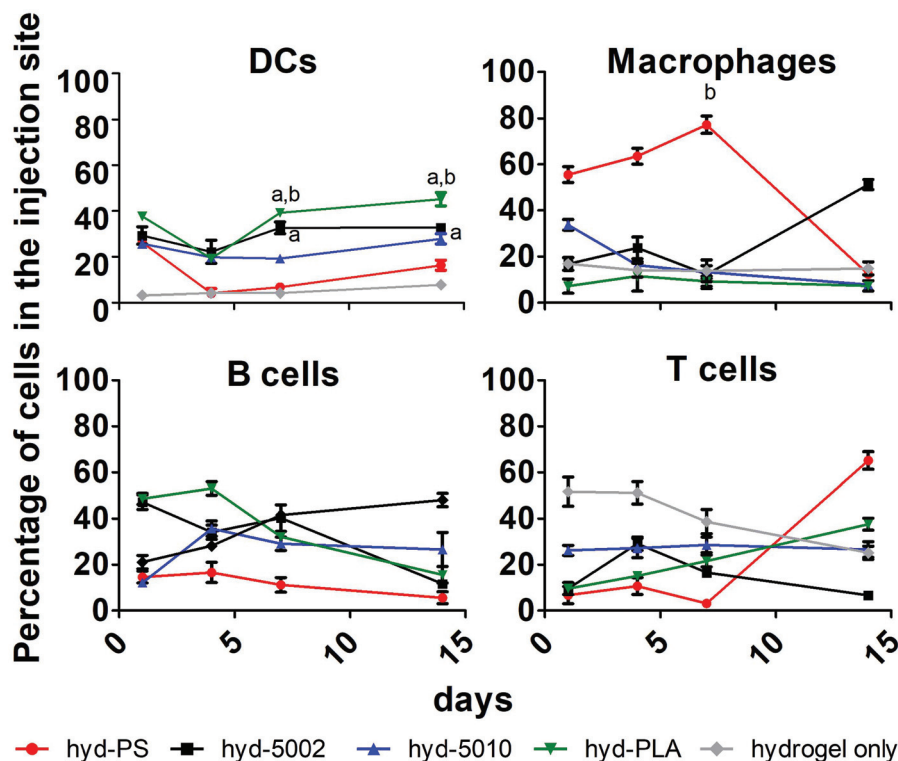
Fig. 3 GM–CSF loaded hydrogels alter the immune cell composition of the subcutaneously implanted hydrogel over time. After 1, 4, 7, and 14 days the implanted PLGA-, PLA-, or PS-loaded hydrogels were extracted and the immune cells in the hydrogels were quantified. B cells, T cells, DCs, and MΦs were identified by their expression of CD19, CD3, CD11c, and F4/80, respectively. Comparisons were drawn to mice that were injected with the Puramatrix hydrogel alone, using a two-way ANOVA. The a represents a statistically significant difference from the hydrogel alone ($p < 0.05$), b represents a statistically significant difference compared to the PS-loaded hydrogel ($p < 0.05$), $n = 3$ biological replicates per formulation per time point.

PLA or hyd-PS. The loss of immunosuppression exerted by lactate at 14 days could be attributed to the degradation of both the hydrogel and its encapsulated MPs. After 14 days, the gel and PLGA MPs are largely degraded, and it became an experimental challenge to isolate and harvest the intact hydrogel and associated cells. This may have contributed to some of the inconsistent results at the final time point.

Interestingly, in the inguinal lymph node, the immediate draining lymph node from the injection site, we also saw downregulation of CD86 on particle-associated DCs from mice injected with hyd-5002 compared to hyd-PS at both 7 and 14 days (Fig. S5†). Interestingly, it has been reported that within tumor draining lymph nodes, DC frequency and maturation status of DCs are diminished.[42] No changes in MHCII expression were seen at any time point in total DCs or particle-associated DCs extracted from the subcutaneously implanted hydrogel.

The disparities in CD86 expression between total DCs in the injection site and particle-associated DCs may be due to the phagocytosis. Once inside the hydrogel, phagocytic cells, such as DCs are able to internalize MPs. Within the phagolysosome, PLGA rapidly breaks down via acid-mediated hydrolysis.[37] This results in a rapid release of lactate inside the cell and seemingly, a subsequent decrease in the expression of CD86. This effect was dependent on the molecular weight of the polymer, as the lower molecular weight polymers (5002 and PLA) break down quicker than the 5010.[37] Alternatively, DCs that did not phagocytose particles are likely exposed to lactic acid through (1) lactate transport across the plasma membrane (of cells that have internalized MPs) via monocarboxylate transporters and, (2) the hydrolysis of unphagocytosed MPs.

Dendritic cells in the degradable, MP-loaded hydrogels displayed a similar immunophenotype to that seen in the TME, as well as to that reported in other 3D models of the TME. Interestingly, Michielsen et al. utilized an explanted human colorectal cancer tissue to model the TME and found that DCs implanted in the explant failed to upregulated CD86, even in the presence of inflammatory stimuli (LPS).[43–45] Moreover, CD86 is also required to reactivate tolerized T cells in the prostate tumor tissue, which may be pertinent to latent downregulation of CD28 and CD40 observed on hydrogel-resident T cells and is further discussed below.[46]

Along with DCs, MΦs play a key role in the immune response to tumors.[47] Tumor-associated MΦs are key cells that help to create an immunosuppressive TME by producing cytokines, chemokines, growth factors, and triggering the release of inhibitory immune checkpoint proteins in T cells.[48]
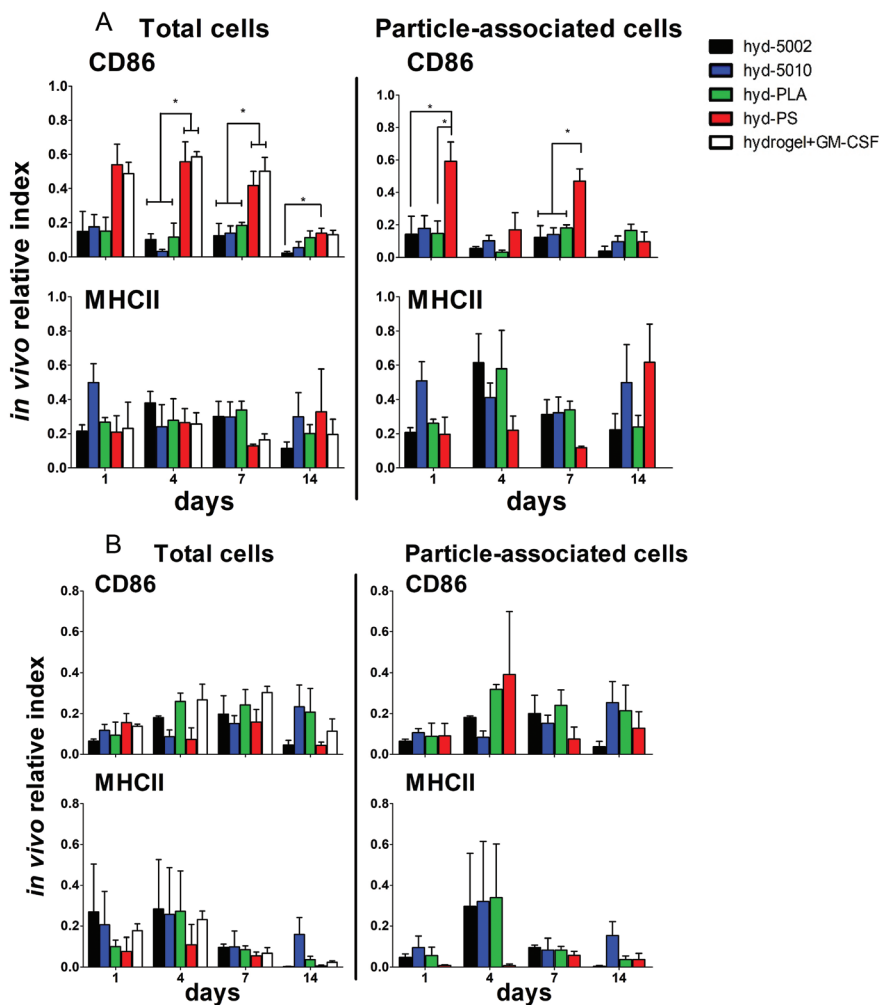
Fig. 4 Peptide hydrogels loaded with degradable PLGA MPs alter the maturation of innate immune cells and mimic the immunosuppressive TME. (A) Dendritic cells and (B) MΦs from the peptide hydrogel were immunophenotyped for their expression of CD86 and MHCII at 1, 4, 7, and 14 days after subcutaneous implantation in C57BL/6J mice. The y-axis denotes the 'in vivo relative index' which is a measure of the number of DCs or MΦs positive for each maturation marker (e.g. # CD86+CD11c+) divided by the total number of each cell type (e.g. # CD11c+). Histograms represent mean and standard error. Total DCs and MΦs and particle-associated DCs and MΦs were analyzed by flow cytometric means. Pair-wise significant differences are denoted by the * symbol ($p \leq 0.05$; $n = 3$ biological replicates).

Therefore, we profiled the expression of CD86 and MHCII on F4/80+ MΦs in the hydrogel injection site (Fig. 4B). Somewhat surprisingly, we did not observe any changes in the maturation status of MΦs at any timepoint when comparing total MΦs and particle-associated MΦs in the PLGA, PLA, or PS-loaded hydrogels. Recent research has shown that lactate indeed polarizes MΦs to a tumor-associated MΦ-like phenotype. However, the pro-tumor qualities of these MΦs may not be associated with their abilities as APCs, but rather as their roles as initiators of chemotaxis.[49] Moreover, the expression of MHC II does not always correlate with antigen presenting ability and further studies may be needed to evaluate how lactate alters antigen presentation, as factors such as antigen processing and subsequent loading onto the MHCII complex can also be altered by the TME.[50,51] Moreover, markers such as CD38, CD206, iNOS, Arginase, which are more characteristic of the

M2 phenotype, may be better identifiers of protumor MΦs than CD86 and MHCII.[52]

Adaptive immune cells from lactate-releasing hydrogels show more a suppressive face

It is a widely held view that the engagement of both innate and adaptive cellular immune responses is necessary for efficient immunotherapy of cancer. Adaptive immune responses are directed against tumor-specific antigens that are not displayed on the surface of normal cells. Given that there was significant infiltration of these hydrogel formulations by B and T cells, we assessed the immune phenotype of adaptive immune cells isolated from the respective hydrogels. Specifically, we evaluated both T and B cells at the injection site, and also analyzed the subset of particle-associated B cells. We were interested in the markers – CD40, MHCII, and CD86

on B cells. CD86 and CD40 are co-stimulatory ligand/receptors on B cells that directly interact with T cells and can promote isotype switching in B cells. MHCII is an antigen presenting moiety, important for antigen-specific activation of B cells. The particle-laden hydrogels did not alter the maturation of B cells after 1 day, as we observed no change in expression of CD40, MHCII, or CD86 within that period (Fig. 5A). However, at longer implantation times, B cell maturation was altered. At 4 days, we saw decreased expression of CD86 on B cells in the injection site in the hyd-5002, hyd-5010 and hyd-PLA, in comparison to the hyd-PS. Further, we saw decreased levels of CD40 on B cells harvested from hyd-5002, hyd-5010, and hyd-PLA, in comparison to hyd-PS.[53] This trend continued for CD40 at the 7- and 14-day time points.

We examined the subset of particle-associated B cells based on the CD19+ and particle-associated double staining. Interestingly, the expression of CD40 on particle-associated B cells in the injection site matched that of total B cells in the injection site. CD40 was downregulated on all particle-associated B cells from hyd-5002, hyd-5010, and hyd-PLA at 4, 7, and 14 days, compared to particle-associated B cells from the hyd-PS. Moreover, we observed a significant decrease in CD86 expression on particle-associated B cells from hyd-5002, hyd-5010, and hyd-PLA, in comparison to particle-associated B cells from hyd-PS on day 7.

We probed the activation status of T cells by looking at the expression of CD28 and CD40L (Fig. 5B). T cells are crucial in the antitumor response, and their inhibition due to tumor-derived lactate is well documented.[12] In general, we observed similar patterns with T cells as those seen with B cells. However, the activation status of T cells was more dependent on PLGA formulation. At the early time points, there were no changes in the expression of CD28 or CD40L. However, at longer incubation times, we observed changes in T cell imune phenotype. For instance, at 7 days after subcutaneous implantation, we saw significant decrease in the expression of CD28 on T cells from the injection site in hyd-5002, compared to both hyd-PS and the hydrogel with GM-CSF only. We did not observe any other changes in CD28 at any other timepoint. At 14 days post implantation, there were significant decreases in the expression of CD40L in T cells harvested from hyd-5002 and hyd-PLA, in comparison to those analyzed from hyd-PS and the hydrogel + GM-CSF formulation. Moreover, we also observed decreased expression of CD40L on T cells taken from the inguinal lymph node of mice that were implanted with hyd-5002, in comparison those take from hyd-PS-injected mice at 14 days after implantation (Fig. S6†).

In general, hydrogel-generated lactate seemed to sway the immune phenotype of B cells more than T cells. Moreover, we postulate that the early decreased expression of CD40 on B cells may account for the delayed, decreased expression of CD40L that occurred after 14 days of implantation. Dampening of CD40-CD40L signaling results in the downregulation of inflammatory markers and increase tolerogenic factor secretion.[54] Moreover, T cells are not phagocytic cells, and thus their exposure to lactate is based on the breakdown of the
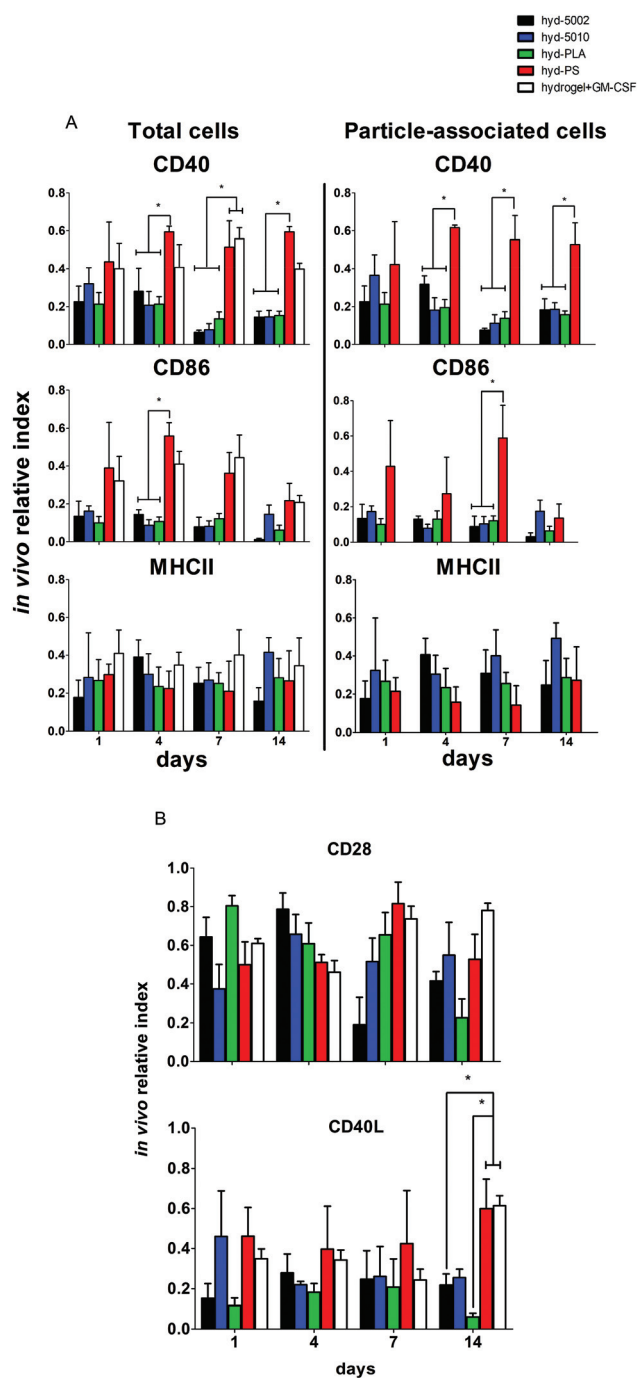

Fig. 5 Polymer-loaded hydrogels influence the activation status of adaptive immune cells through downregulation of key immunostimulatory molecules. (A) Total B cells and particle-associated B cells from hyd-5002, hyd-5010, hyd-PLA, hyd-PS, and unloaded hydrogels were immunophenotyped for their expression of CD40, CD86, and MHCII at 1, 4, 7, and 14 days after subcutaneous implantation in C57BL/6J mice. (B) Total T cells from subcutaneously implanted hydrogels were immunophenotyped for their expression of CD28 and CD40L. Particle-associated cells were not analyzed, as T cells are not phagocytic. The *in vivo* relative index describes the number of T or B cells positive for each maturation marker (*e.g.* # CD28+CD3+) divided by the total number of each cell type (*e.g.* # CD3+). Histograms represent mean and standard error. Statistically significant differences are denoted by the * symbol as determined by a one-way ANOVA at each time point followed by *post hoc* Tukey test ($p < 0.05$), $n = 3$ biological replicates.

MPs inside the hydrogel. This phenomenon may explain the dependence of polymer formulation on CD40L expression at 14 days, as the 5010 formulation has delayed release of lactic acid due to a slower breakdown. With respect to antitumor activity, B cells are multifaceted – they can serve as APCs that drive tumor-specific T cell activation, or mature into plasma cell that secrete tumor-specific antibodies which boost tumor antigen-driven immune responses. The hyd-5002, hyd-5010, and hyd-PLA reduced the expression of CD40 on B cells at 4, 7, and 14 hours. A reduction in CD40 expression has severe consequences for cytotoxic-mediated destruction of tumors. CD40-activated B cells acquire the ability to be potent APCs and drive the antigen-specific response in CD8 T cells. Moreover, CD40-activated B cells, *via* CD40L, can reduce B16. F10 melanoma tumor burden in C57BL/6J mice.[55] Summarily, reduction in the expressions of CD86 in DCs and CD40 on B cells, as seen in the PLGA-hydrogel formulations, can limit the antigen-specific activation of T cells and is a prominent characteristic of cold tumors. With respect to our observations on CD3+ cells harvested from the PLGA and PLA MP-loaded hydrogels, the delayed reduced expression of CD28 and CD40L may be from crosstalk with innate immune cells, primarily DCs, which have a large influence on the polarity of T cells. The results of our work align with others that demonstrate downregulation of CD28 and CD40L on tumor-resident T cells. Recently, Brown *et al.* summised, through RNASeq analysis, that Gpr81 (the primary receptor for lactate on T cells) suppresses the ability of the host immune system to recognize the tumor cells by directly altering the CD28 signaling pathway.[56] Additionally, work from the Bronte group has shown that CD40-CD40L stimulation is necessary to drive the efficacy of T cell cancer therapy.[57]

Conclusions

This work represents the first iteration of an engineered model to understand the immunomodulatory properties of lactate *in vivo*. The PLGA MP-loaded hydrogels recapitulate the immunosuppressive "cold" tumor environment and serve as a proxy for the TME. Lactate accumulation inside the hydrogel, as a result of PLGA breakdown, was comparable to concentrations observed in different tumor types. Moreover, there was infiltration of immune cells into hydrogels, akin to the dynamics seen in tumors. Remarkably, infiltrating immune cells within the hydrogels loaded with lactide-based MPs showed a high degree of immunosuppression, typically at the 7 day time point. These observations are consistent with seminal studies on the immune phenotype of cells within the TME and the role lactate plays. On this basis, we believe this system can be utilized to isolate the effects of lactate on immune cells, and further educate scientists on the pluripotent effects of this ubiquitous metabolite, especially in the context of cancer. Moreover, this hydrogel system holds tremendous potential for further expansion and exploitation as a research tool. Ostensibly, a plurality of factors that contribute to immuno-suppression in the TME (*e.g.* hypoxia) could be easily added to this hydrogel construct for further systems biology-based exploration of immune responses.[58] Facile incorporation of immunotherapeutic drugs into this platform for discovery and mechanistic studies is also within the realm of possibilities.

Conflicts of interest

There are no conflicts of interest.

Acknowledgements

References

1 F. R. Eilber, E. C. Holmes and D. L. Morton, Immunotherapy as an adjunct to surgery in the treatment of cancer, *World J. Surg.*, 1977, **1**(5), 547–554.

2 A. Akinleye and Z. Rasool, Immune checkpoint inhibitors of PD-L1 as cancer therapeutics, *J. Hematol. Oncol.*, 2019, **12**, 92.

3 P. Bonaventura, T. Shekarian, V. Alcazer, J. Valladeau-Guilemond, S. Valsesia-Wittmann, S. Amigorena, *et al.*, Cold Tumors: A Therapeutic Challenge for Immunotherapy, *Front. Immunol.*, 2019, **10**, 168.

4 J. Schlom, J. W. Hodge, C. Palena, K. Y. Tsang, C. Jochems, J. W. Greiner, *et al.*, Therapeutic cancer vaccines, *Adv. Cancer Res.*, 2014, **121**, 67–124.

5 A. Morrot, L. M. da Fonseca, E. J. Salustiano, L. B. Gentile, L. Conde, A. A. Filardy, *et al.*, Metabolic Symbiosis and immunomodulation: How Tumor Cell-Derived Lactate May Disturb innate and Adaptive immune Responses, *Front. Oncol.*, 2018, **8**, 81.

6 M. L. Goodwin, L. B. Gladden, M. W. Nijsten and K. B. Jones, Lactate and cancer: revisiting the warburg effect in an era of lactate shuttling, *Front. Nutr.*, 2014, **1**, 27.

7 D. Raychaudhuri, R. Bhattacharya, B. P. Sinha, C. S. C. Liu, A. R. Ghosh, O. Rahaman, *et al.*, Lactate Induces Pro-tumor Reprogramming in Intratumoral Plasmacytoid Dendritic Cells, *Front. Immunol.*, 2019, **10**, 1878.

8 H. Dong and T. N. Bullock, Metabolic influences that regulate dendritic cell function in tumors, *Front. Immunol.*, 2014, **5**, 24.

9 A. Errea, D. Cayet, P. Marchetti, C. Tang, J. Kluza, S. Offermanns, *et al.*, Lactate Inhibits the Pro-Inflammatory Response and Metabolic Reprogramming in Murine Macrophages in a GPR81-Independent Manner, *PLoS One*, 2016, **11**, 11.

10 E. Gottfried, M. Kreutz, S. Haffner, E. Holler, M. Iacobelli, R. Andreesen, *et al.*, Differentiation of human tumour-associated dendritic cells into endothelial-like cells: An

alternative pathway of tumour angiogenesis, *Scand. J. Immunol.*, 2007, **65**(4), 329–335.

11 Z. Husain, Y. N. Huang, P. Seth and V. P. Sukhatme, Tumor-Derived Lactate Modifies Antitumor Immune Response: Effect on Myeloid-Derived Suppressor Cells and NK Cells, *J. Immunol.*, 2013, **191**(3), 1486–1495.

12 K. Fischer, P. Hoffmann, S. Voelkl, N. Meidenbauer, J. Ammer, M. Edinger, *et al.*, Inhibitory effect of tumor cell-derived lactic acid on human T cells, *Blood*, 2007, **109**(9), 3812–3819.

13 C. Harmon, M. W. Robinson, F. Hand, D. Almuaili, K. Mentor, D. D. Houlihan, *et al.*, Lactate-Mediated Acidification of Tumor Microenvironment Induces Apoptosis of Liver-Resident NK Cells in Colorectal Liver Metastasis, *Cancer Immunol. Res.*, 2019, **7**(2), 335–346.

14 M. E. Katt, A. L. Placone, A. D. Wong, Z. S. Xu and P. C. Searson, In Vitro Tumor Models: Advantages, Disadvantages, Variables, and Selecting the Right Platform, *Front. Bioeng. Biotechnol.*, 2016, **4**, 12.

15 L. DiPersio, A. P. Kyriazis, J. G. Michael and A. J. Pesce, Monitoring the therapy of human tumor xenografts in nude mice by the use of lactate dehydrogenase, *J. Natl. Cancer Inst.*, 1979, **62**(2), 375–379.

16 Z. Liu and G. Vunjak-Novakovic, Modeling tumor microenvironments using custom-designed biomaterial scaffolds, *Curr. Opin. Chem. Eng.*, 2016, **11**, 94–105.

17 P. Beri, B. F. Matte, L. Fattet, D. Kim, J. Yang and A. J. Engler, Biomaterials to model and measure epithelial cancers, *Nat. Rev. Mater.*, 2018, **3**(11), 418–430.

18 F. Bersani, J. Lee, M. Yu, R. Morris, R. Desai, S. Ramaswamy, *et al.*, Bioengineered implantable scaffolds as a tool to study stromal-derived factors in metastatic cancer models, *Cancer Res.*, 2014, **74**(24), 7229–7238.

19 L. J. Bayne, G. L. Beatty, N. Jhala, C. E. Clark, A. D. Rhim, B. Z. Stanger, *et al.*, Tumor-derived granulocyte-macrophage colony-stimulating factor regulates myeloid inflammation and T cell immunity in pancreatic cancer, *Cancer Cell*, 2012, **21**(6), 822–835.

20 Y. M. Yoon, J. S. Lewis, M. R. Carstens, M. Campbell-Thompson, C. H. Wasserfall, M. A. Atkinson, *et al.*, A combination hydrogel microparticle-based vaccine prevents type 1 diabetes in non-obese diabetic mice, *Sci. Rep.*, 2015, **5**, 13155.

21 J. Casey, X. S. Yue, T. D. Nguyen, A. Acun, V. R. Zellmer, S. Y. Zhang, *et al.*, 3D hydrogel-based microwell arrays as a tumor microenvironment model to study breast cancer growth, *Biomed. Mater.*, 2017, **12**(2), 025009.

22 V. Chew, H. C. Toh and J. P. Abastado, Immune microenvironment in tumor progression: characteristics and challenges for therapy, *J. Oncol.*, 2012, **2012**, 608406.

23 T. F. Gajewski, H. Schreiber and Y. X. Fu, Innate and adaptive immune cells in the tumor microenvironment, *Nat. Immunol.*, 2013, **14**(10), 1014–1022.

24 K. G. de la Cruz-Lopez, L. J. Castro-Munoz, D. O. Reyes-Hernandez, A. Garcia-Carranca and J. Manzo-Merino, Lactate in the Regulation of Tumor Microenvironment and Therapeutic Approaches, *Front. Oncol.*, 2019, **9**, 1143.

25 S. Romero-Garcia, M. M. Moreno-Altamirano, H. Prado-Garcia and F. J. Sanchez-Garcia, Lactate Contribution to the Tumor Microenvironment: Mechanisms, Effects on Immune Cells and Therapeutic Relevance, *Front. Immunol.*, 2016, **7**, 52.

26 I. S. Hong, Stimulatory versus suppressive effects of GM-CSF on tumor progression in multiple cancer types, *Exp. Mol. Med.*, 2016, **48**(7), e242.

27 C. Ghirelli, F. Reyal, M. Jeanmougin, R. Zollinger, P. Sirven, P. Michea, *et al.*, Breast Cancer Cell-Derived GM-CSF Licenses Regulatory Th2 Induction by Plasmacytoid Predendritic Cells in Aggressive Disease Subtypes, *Cancer Res.*, 2015, **75**(14), 2775–2787.

28 F. Reggiani and F. Bertolini, GM-CSF promotes a supportive adipose and lung microenvironment in metastatic breast cancer, *Oncoscience*, 2017, **4**(9–10), 126–127.

29 O. A. Ali, N. Huebsch, L. Cao, G. Dranoff and D. J. Mooney, Infection-mimicking materials to program dendritic cells in situ, *Nat. Mater.*, 2009, **8**(2), 151–158.

30 A. Nishimura, T. Hayakawa, Y. Yamamoto, M. Hamori, K. Tabata, K. Seto, *et al.*, Controlled release of insulin from self-assembling nanofiber hydrogel, PuraMatrix: application for the subcutaneous injection in rats, *Eur. J. Pharm. Sci.*, 2012, **45**(1–2), 1–7.

31 A. D. Lynn, A. K. Blakney, T. R. Kyriakides and S. J. Bryant, Temporal progression of the host response to implanted poly(ethylene glycol)-based hydrogels, *J. Biomed. Mater. Res., Part A*, 2011, **96**(4), 621–631.

32 G. Miller, V. G. Pillarisetty, A. B. Shah, S. Lahrs, Z. Xing and R. P. DeMatteo, Endogenous granulocyte-macrophage colony-stimulating factor overexpression in vivo results in the long-term recruitment of a distinct dendritic cell population with enhanced immunostimulatory function, *J. Immunol.*, 2002, **169**(6), 2875–2885.

33 R. Sivakumar, M. Chan, J. S. Shin, N. Nishida-Aoki, H. L. Kenerson, O. Elemento, *et al.*, Organotypic tumor slice cultures provide a versatile platform for immuno-oncology and drug discovery, *OncoImmunology*, 2019, **8**(12), e1670019.

34 K. J. Mylonas, J. Anderson, T. A. Sheldrake, E. E. Hesketh, J. A. Richards, D. A. Ferenbach, *et al.*, Granulocyte macrophage-colony stimulating factor: A key modulator of renal mononuclear phagocyte plasticity, *Immunobiology*, 2019, **224**(1), 60–74.

35 S. Kawano, M. Kojima, Y. Higuchi, M. Sugimoto, K. Ikeda, N. Sakuyama, *et al.*, Assessment of elasticity of colorectal cancer tissue, clinical utility, pathological and phenotypical relevance, *Cancer Sci.*, 2015, **106**(9), 1232–1239.

36 S. R. Caliari and J. A. Burdick, A practical guide to hydrogels for cell culture, *Nat. Methods*, 2016, **13**(5), 405–414.

37 H. K. Makadia and S. J. Siegel, Poly Lactic-co-Glycolic Acid (PLGA) as Biodegradable Controlled Drug Delivery Carrier, *Polymers*, 2011, **3**(3), 1377–1397.

38 A. Schnell, C. Schmidl, W. Herr and P. J. Siska, The Peripheral and Intratumoral Immune Cell Landscape in Cancer Patients: A Proxy for Tumor Biology and a Tool for Outcome Prediction, *Biomedicines*, 2018, **6**, 25.

39 M. Binnewies, E. W. Roberts, K. Kersten, V. Chan, D. F. Fearon, M. Merad, *et al.*, Understanding the tumor immune microenvironment (TIME) for effective therapy, *Nat. Med.*, 2018, **24**(5), 541–550.

40 A. Fialova, S. Partlova, L. Sojka, H. Hromadkova, T. Brtnicky, J. Fucikova, *et al.*, Dynamics of T-cell infiltration during the course of ovarian cancer: the gradual shift from a Th17 effector cell response to a predominant infiltration by regulatory T-cells, *Int. J. Cancer*, 2013, **132**(5), 1070–1079.

41 R. P. Allen, A. Bolandparvaz, J. A. Ma, V. A. Manickam and J. S. Lewis, Latent, Immunosuppressive Nature of Poly (lactic-co-glycolic acid) Microparticles, *ACS Biomater. Sci. Eng.*, 2018, **4**(3), 900–918.

42 A. Gardner and B. Ruffell, Dendritic Cells and Cancer Immunity, *Trends Immunol.*, 2016, **37**(12), 855–865.

43 A. J. Michielsen, A. E. Hogan, J. Marry, M. Tosetto, F. Cox, J. M. Hyland, *et al.*, Tumour tissue microenvironment can inhibit dendritic cell maturation in colorectal cancer, *PLoS One*, 2011, **6**((11), e27944.

44 A. J. Michielsen, S. Noonan, P. Martin, M. Tosetto, J. Marry, M. Biniecka, *et al.*, Inhibition of dendritic cell maturation by the tumor microenvironment correlates with the survival of colorectal cancer patients following bevacizumab treatment, *Mol. Cancer Ther.*, 2012, **11**(8), 1829–1837.

45 A. J. Michielsen, J. N. O'Sullivan and E. J. Ryan, Tumor conditioned media from colorectal cancer patients inhibits dendritic cell maturation, *OncoImmunology*, 2012, **1**(5), 751–753.

46 S. P. Bak, M. S. Barnkob, A. Bai, E. M. Higham, K. D. Wittrup and J. Chen, Differential requirement for CD70 and CD80/CD86 in dendritic cell-mediated activation of tumor-tolerized CD8 T cells, *J. Immunol.*, 2012, **189**(4), 1708–1716.

47 R. C. Dandekar, A. V. Kingaonkar and G. S. Dhabekar, Role of macrophages in malignancy, *Ann. Maxillofac. Surg.*, 2011, **1**(2), 150–154.

48 Y. Lin, J. Xu and H. Lan, Tumor-associated macrophages in tumor metastasis: biological roles and clinical therapeutic applications, *J. Hematol. Oncol.*, 2019, **12**(1), 76.

49 S. Lin, L. Sun, X. Lyu, X. Ai, D. Du, N. Su, *et al.*, Lactate-activated macrophages induced aerobic glycolysis and epithelial-mesenchymal transition in breast cancer by regulation of CCL5-CCR5 axis: a positive metabolic feedback loop, *Oncotarget*, 2017, **8**(66), 110426–110443.

50 N. Caronni, F. Simoncello, F. Stafetta, C. Guarnaccia, J. S. Ruiz-Moreno, B. Opitz, *et al.*, Downregulation of Membrane Trafficking Proteins and Lactate Conditioning Determine Loss of Dendritic Cell Function in Lung Cancer, *Cancer Res.*, 2018, **78**(7), 1685–1699.

51 C. M. Fu and A. M. Jiang, Dendritic Cells and CD8 T Cell Immunity in Tumor Microenvironment, *Front. Immunol.*, 2018, **9**, 3059.

52 H. Cheng, Z. Wang, L. Fu and T. Xu, Macrophage Polarization in the Development and Progression of Ovarian Cancers: An Overview, *Front. Oncol.*, 2019, **9**, 421.

53 B. O. Lee, J. Moyron-Quiroz, J. Rangel-Moreno, K. L. Kusser, L. Hartson, F. Sprague, *et al.*, CD40, but not CD154, expression on B cells is necessary for optimal primary B cell responses, *J. Immunol.*, 2003, **171**(11), 5707–5717.

54 M. F. Jansen, M. R. Hollander, N. van Royen, A. J. Horrevoets and E. Lutgens, CD40 in coronary artery disease: a matter of macrophages?, *Basic Res. Cardiol.*, 2016, **111**(4), 38.

55 K. Wennhold, T. M. Weber, N. Klein-Gonzalez, M. Thelen, M. Garcia-Marquez, G. Chakupurakal, *et al.*, CD40-activated B cells induce anti-tumor immunity in vivo, *Oncotarget*, 2017, **8**(17), 27740–27753.

56 T. P. Brown, P. Bhattacharjee, S. Ramachandran, S. Sivaprakasam, B. Ristic, M. O. F. Sikder, *et al.*, The lactate receptor GPR81 promotes breast cancer growth via a paracrine mechanism involving antigen-presenting cells in the tumor microenvironment, *Oncogene*, 2020, **39**(16), 3292–3304.

57 I. Marigo, S. Zilio, G. Desantis, B. Mlecnik, A. H. R. Agnellini, S. Ugel, *et al.*, T Cell Cancer Therapy Requires CD40-CD40L Activation of Tumor Necrosis Factor and Inducible Nitric-Oxide-Synthase-Producing Dendritic Cells, *Cancer Cell*, 2016, **30**(3), 377–390.

58 V. Petrova, M. Annicchiarico-Petruzzelli, G. Melino and I. Amelio, The hypoxic tumour microenvironment, *Oncogenesis*, 2018, **7**(1), 10.